

The optical absorption spectrum and photofragmentation processes of silver tetramer ion

A. Terasaki¹, S. Minemoto², M. Iseda², and T. Kondow¹

¹ Cluster Research Laboratory, Toyota Technological Institute in East Tokyo Laboratory, Genesis Research Institute, Inc., 717-86 Futamata, Ichikawa, Chiba 272-0001, Japan

² Department of Chemistry, School of Science, University of Tokyo, 7-3-1 Hongo, Bunkyo, Tokyo 113-0033, Japan

Received: 31 August 1998

Abstract. An optical absorption spectrum of a silver tetramer ion, Ag_4^+ , was obtained in the photon-energy range of 2.0–5.2 eV by measuring its photofragmentation action spectrum. Three major absorption peaks were observed at photon energies of about 3.1, 4.0, and 4.3 eV. Each transition has a narrow line width of less than 0.1 eV, indicating a molecular nature of the present cluster ion at low temperature. Fragmentation channels were strongly dependent on excited states; Ag_3^+ was the dominant product ion at 3.1 and 4.0 eV excitation, whereas only Ag_2^+ was produced at 4.3 eV excitation. The fragmentation was found to proceed in a nonstatistical manner. These processes were further characterized by translational kinetic energies of the photofragments evaluated by the measurements of velocity distributions of neutral fragments. It was shown that photofragments are emitted with relatively low translational energies and that, consequently, they are highly excited in internal modes.

PACS. 36.40.Vz Optical properties of clusters – 36.40.Qv Stability and fragmentation of clusters – 33.20.Lg Ultraviolet spectra

1 Introduction

Optical properties of metal clusters provide fundamental information for investigating their electronic and geometric structures. Extensive studies have been performed on these issues to clarify the novel properties of metal clusters that can be distinguished from bulk-phase properties [1,2]. At an early stage, size dependence of electronic structures was emphasized; the metallic features emerge as the cluster size increases. For these studies, optical absorption spectroscopy has been a powerful technique. The photodepletion technique has been frequently applied to dilute systems such as gas-phase clusters. Initial studies have been focused on sodium clusters, which have been shown to exhibit an optical transition from a collective excitation of valence electrons to a surface-plasma oscillation [3]. For small sodium clusters with sizes of less than about 8 atoms, on the other hand, it was found that their absorption spectra are much more like that of a molecule, which exhibit discrete excited states [4]. These spectra of the small sodium clusters were interpreted by theoretical studies based on quantum chemical calculation [5]. Recently it has been found, in the careful studies of sodium cluster ions [6–8], that the electronic structure of a metal cluster depends not only on its size but also on its internal energy (temperature). This

finding points out the importance of vibronic couplings in metal cluster systems. However, it still remains to be clarified if this temperature-dependent behavior is common to other metal clusters, and how a molecular nature changes to a metallic one at an intermediate temperature regime.

Among metal clusters, silver clusters are attracting attention because of their important physical and chemical properties, e.g., their catalytic role in photography [9]. Since both silver and sodium are monovalent elements, it is meaningful to compare the properties of silver clusters with those of sodium clusters. Optical properties of silver clusters have been studied in this respect. A giant resonance due to surface-plasma excitation has been observed in relatively hot clusters generated from a sputtering cluster-ion source [10–12]. Silver clusters in a rare-gas matrix have also been shown to exhibit a collective excitation of the valence electrons [13, 14]. These results have been interpreted on the basis of the shell model. Recently, optical absorption spectra of relatively cold silver clusters in the gas phase have been reported [15, 16]. There was an indication of a molecular feature of these clusters, but the measured spectral range was limited. Theoretical studies have also been performed to determine the geometric structures of neutral, cationic [17], and anionic [18] silver clusters. Furthermore, dynamical processes are gaining an interest in

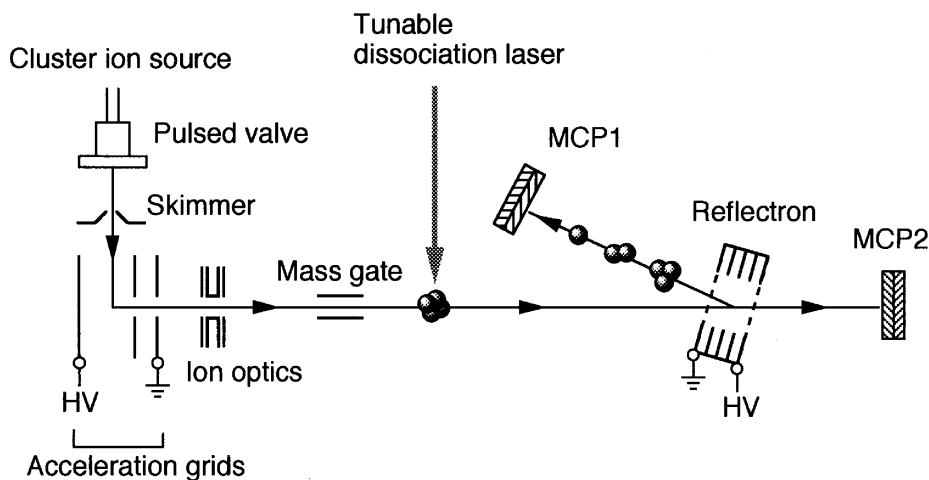


Fig. 1. Schematics of the experimental setup. HV: High-voltage power supply; MCP: Microchannel plate.

the recent time-resolved studies by the so-called NeNePo scheme [19, 20].

In the present paper, we report an absorption spectrum of a silver tetramer ion generated by laser vaporization at a relatively low temperature. It was obtained by measuring a photofragmentation action spectrum in a wide spectral range of 2.0–5.2 eV, and its electronic states were scrutinized. As for the dynamical aspects, the fragmentation pathways and the redistribution processes of excess energies are discussed on the basis of energetics and dynamics in the excited states.

2 Experimental procedures

Figure 1 shows a schematic diagram of the experimental setup. Silver cluster ions, Ag_n^+ , were produced by the laser vaporization technique, which entailed the use of the second harmonics of a Q-switched Nd:YAG laser. Cluster ions thus produced were skimmed (1 mm in diameter) and extracted by a pulsed electric field. The cluster ions gained a kinetic energy of 1400 eV. After passing through a mass gate, a tunable dissociation laser pulse from an optical parametric oscillator (Spectra Physics, MOPO-730) was irradiated at a right angle to a tetramer ion, Ag_4^+ , mass-selected by time-of-flight (TOF). Photofragment ions and residual parent ions were mass-analyzed by the second TOF path using a reflectron and detected by a microchannel plate (MCP1). Neutral photofragments penetrated through the reflectron were detected by the second microchannel plate (MCP2) located downstream by 0.9 m from the laser-interaction region. TOF spectra were stored either in a transient digitizer (Iwatsu, DM2300) or in a multichannel scaler (Stanford Research Systems, SR430), and were processed by a personal computer (NEC, PC-9801VX). The measurement was performed at the repetition rate of 10 Hz.

By measuring the intensity of photofragment ions Ag_n^+ ($n = 1, 2, \text{ and } 3$) relative to the parent ion and that of an irradiated laser pulse (typically $1\text{--}5 \text{ mJ cm}^{-2} \text{ pulse}^{-1}$), a cross section of each fragmentation channel was obtained.

The laser beam was collimated to a spot size of about 5 mm in diameter and was timed carefully to precisely overlap with all the isotopomers in the cluster-ion pulse. Since a silver atom has isotopes of ^{107}Ag and ^{109}Ag with almost the same abundance, there appear five peaks in the mass spectrum of Ag_4^+ corresponding to different combinations of the isotopes. The photon energy was varied from 2.0 to 5.2 eV. A total cross section was obtained as a sum over cross sections of all the fragmentation channels; it corresponds to an optical absorption cross section under the likely assumption that all the photoexcited cluster ions are dissociated within a time scale of observation, about $30 \mu\text{s}$.

For evaluation of translational kinetic energies released upon photofragmentation, TOF spectra of neutral fragments were measured. In this experiment, the dissociation laser pulse was focused by a cylindrical lens with a 500 mm focal length, which produced an ellipsoidal beam profile with a longer (vertical) and shorter (horizontal) diameter of about 5 mm and 1 mm, respectively. With this arrangement, the laser pulse could illuminate one of the isotopomers. Measurements were performed on two isotopomers, $^{107}\text{Ag}_4^+$ and $(^{107}\text{Ag}_2^{109}\text{Ag}_2)^+$. They gave almost identical results, which verified that an isotope effect on the TOF was negligibly small. The kinetic-energy spread of the parent ion beam was measured to be about 12 eV in the laboratory frame by both TOF broadening and ion-intensity change with retarding voltage applied to the reflectron. This energy spread was much narrower than the observed broadening of a neutral fragment. The polarization plane of the laser beam was fixed to be either parallel or perpendicular to the cluster-ion beam.

The temperature of the present cluster ion was estimated by the measurement of the unimolecular dissociation rate of an argon-atom adduct, Ag_4^+Ar , produced from the same cluster-ion source by the use of a carrier gas of a 10% mixture of argon in helium. No unimolecular dissociation was observed in the present experimental time scale of about $60 \mu\text{s}$. If the binding energy of the argon atom to Ag_4^+ is assumed to be 0.07 eV, which has been reported for the physisorption energy of an argon atom on a bulk silver surface [21], this sets an upper bound of about 150 K for the temperature of the tetramer ion.

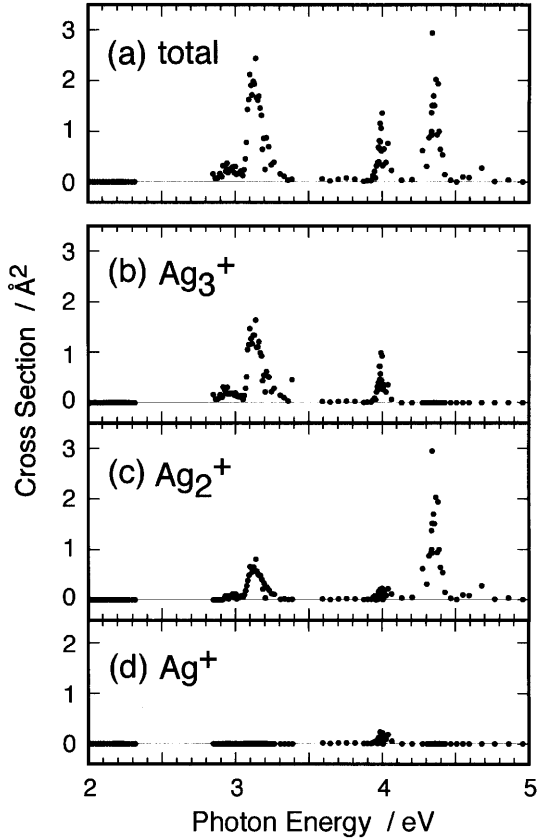


Fig. 2. Cross sections of photofragment-ion production from Ag_4^+ as a function of the photon energy. The photofragment ion is (b) Ag_3^+ , (c) Ag_2^+ , and (d) Ag^+ . Panel (a) shows a total cross section obtained as the sum over three fragmentation channels, which corresponds to an absorption spectrum.

3 Results

As shown in Fig. 2(a), three major absorption peaks were observed. By fitting each peak with a Gaussian profile, these peaks were found to be centered at 3.13, 4.00, and 4.36 eV and to have line widths of less than 0.1 eV in full width at half maximum (FWHM). The corresponding oscillator strengths were estimated to be about 0.3, 0.1, and 0.2, respectively. The uncertainty in the absolute cross section was estimated to be $\pm 25\%$, due mainly to the uncertainty in the evaluation of an interaction volume between a laser pulse and a cluster ion. Figure 2(b)–2(d) show cross sections of each fragmentation channel for the production of Ag_3^+ , Ag_2^+ , and Ag^+ as a function of the photon energy. The fragmentation pattern was strongly dependent on the excitation energy: At about 3.1 and 4.0 eV, Ag_3^+ was produced dominantly with much smaller amounts of Ag_2^+ and Ag^+ . On the other hand, only Ag_2^+ was a product ion at about 4.3 eV.

TOF spectra of neutral fragments were obtained at three different photon energies corresponding to each absorption peak: 3.11, 4.01, and 4.36 eV. The TOF was converted to a velocity component parallel to the cluster-ion beam in the center-of-mass frame (a parallel velocity, v_{\parallel}).

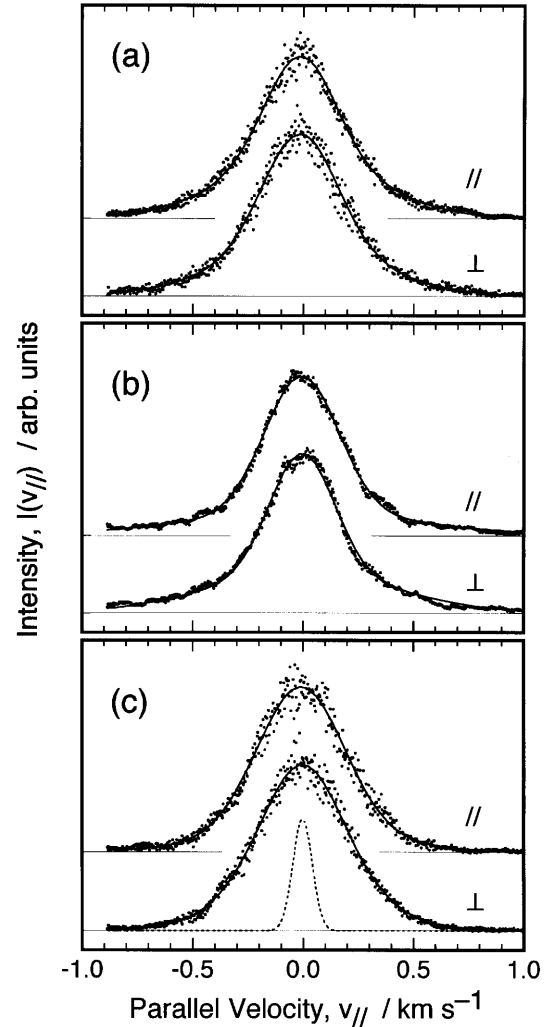


Fig. 3. Intensities of neutral photofragments, $I(v_{\parallel})$, as a function of the velocity component, v_{\parallel} , parallel to the cluster-ion beam in the center-of-mass frame. Photon energies are (a) 3.11 eV, (b) 4.01 eV, and (c) 4.36 eV. The polarization plane of the laser beam was either parallel (//) or perpendicular (\perp) to the cluster-ion-beam axis. Solid curves represent simulations of each profile by a sum of two Gaussian functions. A dashed line in panel (c) shows a velocity distribution of the parent cluster ion.

Distributions thus obtained for the parallel velocities of the neutral fragments are shown in Fig. 3. These profiles are symmetric with respect to $v_{\parallel} = 0$ and have no significant dependence on the polarization plane of the dissociation laser beam. These results indicate that photofragments are emitted isotropically from the parent cluster ion. All the profiles are significantly broadened, compared with the initial velocity distribution of the parent cluster ion shown by a dashed line in Fig. 3(c). Therefore, the broadening is predominantly due to the kinetic-energy distribution of the neutral fragments. The relatively narrow transition line widths and the isotropic emission of fragments imply a predissociative nature of the present photofragmentation process.

4 Discussion

4.1 Assignment of transitions

The absorption spectrum shown in Fig. 2(a) has relatively narrow line widths, of less than 0.1 eV in FWHM, when compared with those obtained in the previous studies on Ag_n^+ and Ag_n^- produced by a sputtering cluster-ion source [10–12]. The latter spectra have line widths broader than 0.5 eV, and are interpreted to originate from a collective excitation of electrons in the surface-plasmon mode observed in hot clusters. On the other hand, the silver tetramer ion under discussion is at a temperature lower than 150 K, which means it can be regarded to be in a molecule-like state rather than in a metallic state with delocalized valence electrons. It should be pointed out that the present spectrum is similar to that of Na_4^+ at low temperatures [6–8]; there are three major peaks in this photon-energy range, although peaks are shifted by about 1 eV to a higher-energy side in Ag_4^+ . Because it has been shown theoretically that Ag_4^+ and Na_4^+ have the same symmetry of D_{2h} (a rhombic structure) at the optimized structure in the ground state [8, 17], it is reasonable that Ag_4^+ have an electronic structure similar to that of Na_4^+ . Therefore, we assume that these transitions have origins similar to the corresponding transitions of Na_4^+ : The ground state is $^2B_{1u}$, and the excited states at 3.1, 4.0, and 4.3 eV are 2A_g , $^2B_{3g}$, and $^2B_{2g}$, respectively.

4.2 Fragmentation pathways

As shown in Fig. 2, fragmentation channels depend on excited states. These fragmentation pathways can be assigned on the basis of energetics. The relevant dissociation energies are predicted by theoretical calculations as follows [17]: $D(\text{Ag}_3^+ \dots \text{Ag}) = 1.27$ eV, $D(\text{Ag}_2^+ \dots \text{Ag}_2) = 2.56$ eV, $D(\text{Ag}^+ \dots \text{Ag}_3) = 3.22$ eV, and $D(\text{Ag}_2^+ \dots \text{Ag}) = 2.89$ eV.

- 3.1 eV excitation: As shown in Fig. 2, Ag_3^+ and Ag_2^+ are produced. Production of Ag_2^+ is considered to be either a sequential process, i.e., $\text{Ag}_4^+ \rightarrow \text{Ag}_3^+ + \text{Ag} \rightarrow \text{Ag}_2^+ + 2\text{Ag}$, or a direct process, i.e., $\text{Ag}_4^+ \rightarrow \text{Ag}_2^+ + \text{Ag}_2$. From an energetic consideration, the former process requires 4.16 eV, which is not accessible by the photon energy. Therefore, only the latter process is allowed. The branching fraction between Ag_3^+ and Ag_2^+ production provides information about the potential-energy surface in the excited state.
- 4.0 eV excitation: By a similar energetic consideration, all the processes for the production of Ag_3^+ , Ag_2^+ , and Ag^+ are direct processes, i.e., $\text{Ag}_4^+ \rightarrow \text{Ag}_3^+ + \text{Ag}$, $\text{Ag}_4^+ \rightarrow \text{Ag}_2^+ + \text{Ag}_2$, and $\text{Ag}_4^+ \rightarrow \text{Ag}^+ + \text{Ag}_3$, respectively.
- 4.3 eV excitation: Only Ag_2^+ was observed at this photon energy, which is produced via $\text{Ag}_4^+ \rightarrow \text{Ag}_2^+ + \text{Ag}_2$. If the fragmentation process is dominated by a statistical process, i.e., evaporation of neutral products, Ag_3^+

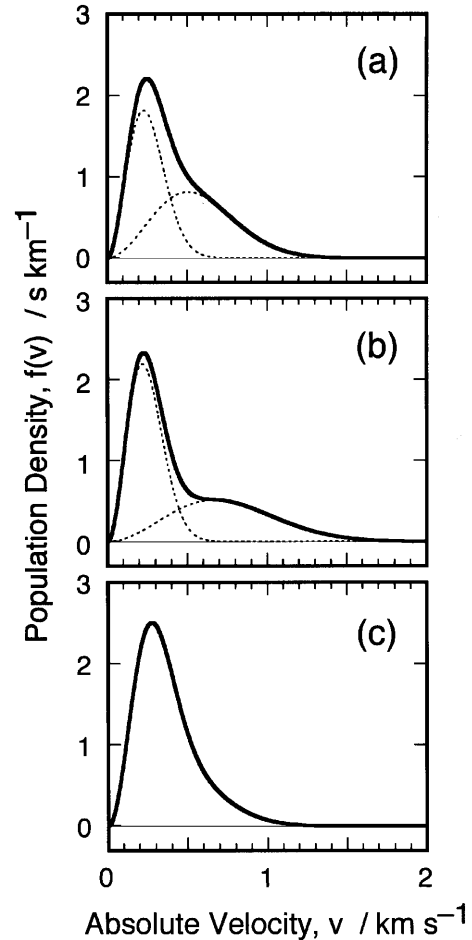


Fig. 4. Absolute-velocity distributions, $f(v)$, of neutral photo-fragments obtained from the parallel-velocity distributions in Fig. 3 (see text). Photon energies are (a) 3.11 eV, (b) 4.01 eV, and (c) 4.36 eV. Dashed lines in (a) and (b) show contributions of two components.

should be observed, because it is more likely to be produced energetically. Therefore, the exclusive production of Ag_2^+ clearly shows a nonstatistical fragmentation process along a potential-energy surface in the excited state. This is in marked contrast to that reported for larger sizes, Ag_9^+ and Ag_{21}^+ , for which dissociation processes were interpreted by a statistical model [22].

4.3 Energy redistribution upon photofragmentation

The one-dimensional parallel-velocity distribution, $I(v_{\parallel})$, of the neutral fragments shown in Fig. 3 can be converted to a three-dimensional velocity distribution, $f(v)$, where v is the absolute velocity in the center-of-mass frame. When fragmentation takes place isotropically as in the present case, a mathematical analysis of this process derives the following relationship:

$$f(v) = -2v \frac{d}{dv_{\parallel}} I(v_{\parallel}) \Big|_{v_{\parallel}=v} ; \quad v > 0. \quad (1)$$

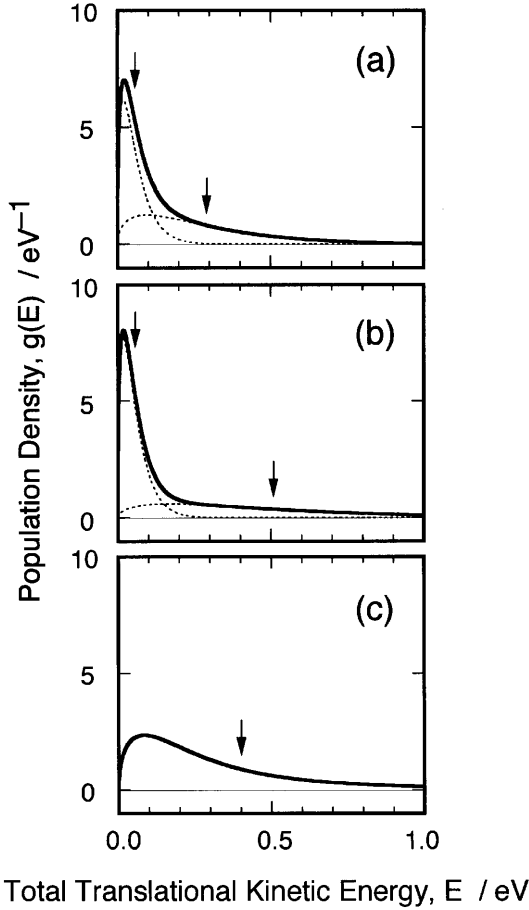


Fig. 5. Distributions, $g(E)$, of translational kinetic energies carried by both a fragment ion and a neutral. Photon energies are (a) 3.11 eV, (b) 4.01 eV, and (c) 4.36 eV. The fragmentation channel was assumed as follows: (a, b) $\text{Ag}_4^+ \rightarrow \text{Ag}_3^+ + \text{Ag}$; (c) $\text{Ag}_4^+ \rightarrow \text{Ag}_2^+ + \text{Ag}_2$. Dashed lines in (a) and (b) show contributions of two components. Arrows indicate an average energy, $\langle E \rangle$, for each component.

In order to obtain $f(v)$, the profiles of $I(v_{\parallel})$ were simulated by a sum of two Gaussian functions centered at $v_{\parallel} = 0$, as shown by solid curves in Fig. 3. They reproduce the obtained data well. Then one obtains $f(v)$ by using the derivatives of these curves according to (1); these are shown in Fig. 4. One should note that the velocity distribution consists of two components in Fig. 4(a) and 4(b), which are illustrated by dashed lines, while that in Fig. 4(c) appears to consist of a single component. From these distribution profiles one obtains an average velocity defined by root-mean-square of the fragment velocity, $(\langle v^2 \rangle)^{1/2}$, where $\langle \rangle$ denotes an averaging over the distribution function, $f(v)$. The average velocities thus obtained for each component are (a) 0.28 and 0.62, (b) 0.27 and 0.82, and (c) 0.42 km/s for 3.11, 4.01, and 4.36 eV excitation, respectively. The velocity distribution can be further translated to a distribution, $g(E)$, of total translational kinetic energy, E , carried both by a neutral photofragment and by a counter ion when the size of the products are given. Figure 5 illustrates profiles of $g(E)$ obtained in the following procedures:

- (a) 3.11 eV excitation: Since the process $\text{Ag}_4^+ \rightarrow \text{Ag}_3^+ + \text{Ag}$ dominates the fragmentation, a distribution, $g(E)$, is obtained as shown in Fig. 5(a). An average total translational kinetic energy, $\langle E \rangle$, of Ag_3^+ and Ag , is calculated to be 0.06 and 0.29 eV in the center-of-mass frame for the slow and the fast components, respectively. Since the corresponding dissociation energy, $D(\text{Ag}_3^+ \dots \text{Ag})$, is reported to be 1.27 eV, the excess energy is 1.84 eV. That is, an average energy as high as 1.78 and 1.55 eV is transferred to the fragment ion, Ag_3^+ , at the slow and the fast fragment velocities, respectively. The trimer ion, Ag_3^+ , is bound so strongly, i.e., $D(\text{Ag}_2^+ \dots \text{Ag}) = 2.89$ eV, that it does not dissociate further, but stays in highly excited vibrational levels. If the vibrational frequency of 161 cm^{-1} measured on Ag_3 [23] is assumed for three vibrational modes of Ag_3^+ , these internal energies simply correspond to vibrational quantum numbers of 30 and 26, respectively, for the slow and the fast components of the neutral fragment.
- (b) 4.01 eV excitation: The process $\text{Ag}_4^+ \rightarrow \text{Ag}_3^+ + \text{Ag}$ is predominant, as in the case above, and $g(E)$ is obtained as shown in Fig. 5(b). The translational kinetic energy of the slow (fast) component is calculated to be an average of 0.06(0.51) eV. This indicates that 2.68(2.23) eV is transferred to the fragment ion, Ag_3^+ , which is even higher than that in the 3.11 eV excitation. Under the same assumption for the vibrational frequency of Ag_3^+ , the vibrational quantum number is estimated to be 45(37).
- (c) 4.36 eV excitation: Only the process $\text{Ag}_4^+ \rightarrow \text{Ag}_2^+ + \text{Ag}_2$ proceeds in this excitation. The distribution function shown in Fig. 5(c) has a smaller low-energy component when it is compared with the other two cases, (a) and (b). The total translational kinetic energy carried by Ag_2^+ and Ag_2 is 0.40 eV in average. From consideration of the excess energy of 1.80 eV, 1.40 eV is transferred to internal energies of both Ag_2^+ and Ag_2 . If the internal energy is assumed to be partitioned equally to both dimers, their vibrational quantum numbers are estimated to be 37 and 52 in Ag_2 and Ag_2^+ , respectively, by using the ground-state vibrational constants reported in [17].

Regarding the origin of the bimodal behavior of the velocity distribution observed at 3.11 and 4.01 eV excitation, the two components can be interpreted to correspond to different atomic sites of the released silver atom: The ground-state geometric structure of Ag_4^+ has been calculated to be rhombic [17]. This character in the geometry is considered to be reflected also in the excited states. When an atom located at the shorter diagonal apex is released, the corresponding fragment ion, Ag_3^+ , is largely distorted from an equilateral triangle structure, which is reported to be the most stable structure of Ag_3^+ in the ground state [17]. Therefore, it is reasonable that Ag_3^+ thus produced is highly excited in vibrational modes. In contrast, when an atom at longer diagonal apex is released, the geometric structure of Ag_3^+ produced is much closer to an equilateral triangle and hence there is lower exci-

tation in internal modes. A further quantitative analysis on the branching ratio is needed to verify this interpretation. Experimental determination of the internal state of the fragment remains for future study, which provides us with important information to characterize these fragmentation processes.

5 Conclusion

The optical absorption spectrum of Ag_4^+ was obtained in the photon-energy range of 2.0–5.2 eV. The spectrum consists of three major peaks at about 3.1, 4.0, and 4.3 eV, with narrow line widths of less than 0.1 eV. This indicates a molecular nature of the present cluster ion at a low temperature. The excited states were assigned in reference to those reported for Na_4^+ . The fragmentation pathways exhibited marked dependence on the excited states. They were assigned by the consideration of energetics. Particularly, the present photofragmentation was found to proceed in a nonstatistical manner. These processes were further characterized by the measurement of translational kinetic energies released. Average translational kinetic energies were found to range from 0.06 to 0.51 eV, depending on the excitation-photon energy and the fragmentation channel. These energies are less than 20% of the excess energy. This indicates that photofragments are highly excited in internal modes. The bimodal behavior observed in the kinetic energies of fragment silver atoms is probably originates from the nonequivalent atomic sites in the parent cluster ion. The present results are expected to motivate theoretical studies and time-resolved experiments by ultrashort laser spectroscopy to further clarify details of the dynamics in the excited states.

The present study was supported by the Genesis Research Institute, Inc.

References

1. W.A. de Heer: *Rev. Mod. Phys.* **65**, 611 (1993)
2. U. Kreibig, M. Vollmer: *Optical Properties of Metal Clusters* (Springer, Berlin 1995).
3. K. Selby, M. Vollmer, J. Masui, V. Kresin, W.A. de Heer, W.D. Knight: *Phys. Rev. B* **40**, 5417 (1989)
4. C.R.C. Wang, S. Pollack, D. Cameron, M.M. Kappes: *J. Chem. Phys.* **93**, 3787 (1990)
5. V. Bonačić-Koutecký, P. Fantucci, J. Koutecký: *J. Chem. Phys.* **93**, 3802 (1990)
6. C. Ellert, M. Schmidt, C. Schmitt, T. Reiners, H. Haberland: *Phys. Rev. Lett.* **75**, 1731 (1995)
7. C. Ellert, M. Schmidt, T. Reiners, H. Haberland: *Z. Phys. D* **39**, 317 (1997)
8. V. Bonačić-Koutecký, J. Pittner, C. Fuchs, P. Fantucci, M.F. Guest, J. Koutecký: *J. Chem. Phys.* **104**, 1427 (1996)
9. T. Leisner, Ch. Rosche, S. Wolf, F. Granzer, L. Wöste: *Surf. Rev. Lett.* **3**, 1105 (1996)
10. J. Tiggesbäumker, L. Köller, H.O. Lutz, K.-H. Meiwes-Broer: *Chem. Phys. Lett.* **190**, 42 (1992)
11. J. Tiggesbäumker, L. Köller, K.-H. Meiwes-Broer, A. Liebsch: *Phys. Rev. A* **48**, R1749 (1993)
12. J. Tiggesbäumker, L. Köller, K.-H. Meiwes-Broer: *Chem. Phys. Lett.* **260**, 428 (1996)
13. W. Harbich, S. Fedrigo, J. Buttet: *Chem. Phys. Lett.* **195**, 613 (1992)
14. S. Fedrigo, W. Harbich, J. Buttet: *Phys. Rev. B* **47**, 10706 (1993)
15. B.A. Collings, K. Athanassenas, D.M. Rayner, P.A. Hackett: *Chem. Phys. Lett.* **227**, 490 (1994)
16. S. Haupt, J. Kaller, D. Schoof, D. Cameron, M.M. Kappes: *Z. Phys. D* **40**, 331 (1997)
17. V. Bonačić-Koutecký, L. Češpiva, P. Fantucci, J. Koutecký: *J. Chem. Phys.* **98**, 7981 (1993)
18. V. Bonačić-Koutecký, L. Češpiva, P. Fantucci, J. Pittner, J. Koutecký: *J. Chem. Phys.* **100**, 490 (1994)
19. S. Wolf, G. Sommerer, S. Rutz, E. Schreiber, T. Leisner, L. Wöste, R.S. Berry: *Phys. Rev. Lett.* **74**, 4177 (1995)
20. D.W. Boo, Y. Ozaki, L.H. Andersen, W.C. Lineberger: *J. Phys. Chem. A* **101**, 6688 (1997)
21. G. Vidali, G. Ihm, H.-Y. Kim, M.W. Cole: *Surf. Sci. Rep.* **12**, 133 (1991)
22. M. Lindinger, K. Dasgupta, G. Dietrich, S. Krückeberg, S. Kuznetsov, K. Lützenkirchen, L. Schweikhard, C. Walther, J. Ziegler: *Z. Phys. D* **40**, 347 (1997)
23. P.Y. Cheng, M.A. Duncan: *Chem. Phys. Lett.* **152**, 341 (1988)
24. V. Bonačić-Koutecký, J. Pittner, M. Boiron, P. Fantucci: *J. Chem. Phys.* **110**, 3876 (1999)

Note added in proof

Recently Bonačić-Koutecký *et al.* reported theoretical calculations of optical absorption spectra of small silver clusters and their ions [24]. The result for the most stable tetramer ion with D_{2h} symmetry reproduces our present spectrum very well. Thus its geometric structure was determined to be rhombic and the observed excited electronic states were assigned.